

Convective Boiling of R-134a in a Bundle of Smooth Tubes

Jung-Oh Kim*, Jin-Pyo Cho*, Nae-Hyun Kim** and Kuk-Kwang Choi**

Key words: Tube bundle, Flow boiling, Convective boiling, R-134a, Heat transfer coefficient

Abstract

In this study, flow boiling experiments were performed using R-134a on a plain tube bundle. Tests were conducted for the following range of variables; quality from 0.1 to 0.9, mass flux from $8 \text{ kg/m}^2\text{s}$ to $26 \text{ kg/m}^2\text{s}$ and heat flux from 10 kW/m^2 to 40 kW/m^2 . The heat transfer coefficients were strongly dependent on the heat flux. However, they were almost independent on the mass flux or quality. The data are compared with the modified Chen model, which predicted satisfactorily ($\pm 30\%$) the data. The Original Chen model, however, did not adequately predict the effect of quality. The reason may be attributed to the flow pattern of the present test, where the bubbly flow prevailed for the entire test range. The heat transfer coefficients of the tube bundle were 6~40% higher than those of the single tube pool boiling.

Nomenclature

A : heat transfer area, πDL [m^2]
 c_{pr} : specific heat of the refrigerant [J/kgK]
 D : tube outer diameter [m]
 F : two-phase multiplier [dimensionless]
 G : mass velocity [$\text{kg/m}^2\text{s}$]
 h : heat transfer coefficient [$\text{W/m}^2\text{K}$]
 h_{fc} : forced convective heat transfer coefficient [$\text{W/m}^2\text{K}$]
 j_g : superficial gas velocity, Gx/ρ_g [m/s]
 j_l : superficial liquid velocity, $G(1-x)/\rho_l$ [m/s]
 k : thermal conductivity [W/mK]

\dot{m}_r : mass flow rate of the refrigerant [kg/s]
 N : number of active heaters upstream of the instrumented tube [dimensionless]
 P : pressure [Pa]
 Pr : Prandtl number [dimensionless]
 P_t : tube pitch [m]
 q'' : heat flux [W/m^2]
 Q_H : heat supplied to a single heater in the test section [W]
 Q_p : heat supplied to the pre-heater [W]
 S : boiling suppression factor
 $T_{p,in}$: refrigerant temperature at the pre-heater inlet [K]
 $T_{p,sat}$: saturation temperature at the pre-heater [K]
 T_{sat} : saturation temperature [K]
 T_w : tube wall temperature [K]

* Graduate School, University of Incheon, Incheon 402-040, Korea

** Department of Mechanical Engineering, University of Incheon, Incheon 402-040, Korea

x : vapor quality [dimensionless]

Greek symbols

Φ_g^2 : two-phase friction multiplier

ρ_g : vapor density [kg/m^3]

ρ_l : liquid density [kg/m^3]

σ : surface tension [N/m]

1. Introduction

Understanding the shell-side flow boiling heat transfer characteristics is important for the design of flooded evaporators. The schematic drawing of a flooded refrigerant evaporator is illustrated in Fig. 1. A refrigerant evaporates on the shell-side by a hot water flowing in the tube-side. Previous studies on the refrigerant flow boiling in smooth tube bundles are summarized in Table 1. Table 1 reveals that most of the studies were conducted at a low quality region using R-113. Only Webb and Chien's⁽⁷⁾ study covers a wide quality.

Most of the flow boiling heat transfer correlations of today have been developed based on in-tube boiling data, and usage of the correlations to bundle flow boiling needs special attention. Webb and Gupte⁽⁸⁾ suggested a Chen-type⁽⁹⁾ correlation because it has been developed based on a sound physical argument. Even for

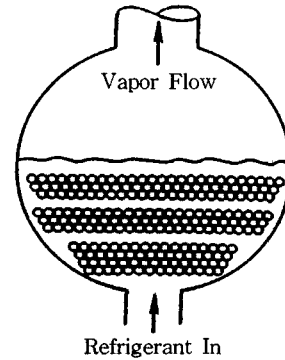


Fig. 1 Schematic of the flooded refrigeration evaporator.

this case, the boiling suppression factor 'S' and two-phase multiplier 'F' may be different from those of in tube flow boiling. In this study, flow boiling experiments were conducted in a smooth bundle using a new refrigerant R-134a. Test ranges were determined considering the operation range of turbo-refrigerator. The quality was varied from 0.1 to 0.9, the mass flux was varied from $8 \text{ kg}/\text{m}^2\text{s}$ to $26 \text{ kg}/\text{m}^2\text{s}$, and the heat flux was varied from $10 \text{ kW}/\text{m}^2$ to $40 \text{ kW}/\text{m}^2$. Test data are compared with the correlation proposed by Webb and Gupte.⁽⁸⁾

2. Experimental apparatus

A schematic drawing of the apparatus is shown in Fig. 2 and the detailed drawing of

Table 1 Summary of data on flow boiling on horizontal, plain tube bundles

Set	Investigators	D	P_t/D	Layout	Fluid	x (%)	q'' (kW/m^2)	G ($\text{kg}/\text{m}^2\text{s}$)	P (bar)
1	Polley et al. ⁽¹⁾	25.4	1.25	Inline	R-113	0-17	10-60	90-450	1
2	Hwang and Yao ⁽²⁾	19.1	1.5	Inline	R-113	1-14	1-30	0-817	1
3	Jensen and Hsu ⁽³⁾	8	1.3	Inline	R-113	0-36	1.6-44.1	50-675	2-5
4	Reinke and Jensen ⁽⁴⁾	7.94	1.3	Stagg	R-113	0-45	1.6-50.5	50-700	2-5
5	Cornwell and Scoones ⁽⁵⁾	25	1.5	Inline	R-113	0-34	5.6-36	150-600	1
6	Jensen et al. ⁽⁶⁾	1.91	1.17	Stagg	R-113	0-80	5-80	50-500	2-6
7a	Webb and Chien ⁽⁷⁾	16.8	1.42	Stagg	R-113	0-90	13-53	7-41	0.45-0.7
7b	Webb and Chien ⁽⁷⁾	16.8	1.42	Stagg	R-123	0-90	13-53	7-16	0.73-1.5
8	Present work	18.8	1.27	Stagg	R-134a	0-90	10-40	8-26	0.34-0.7

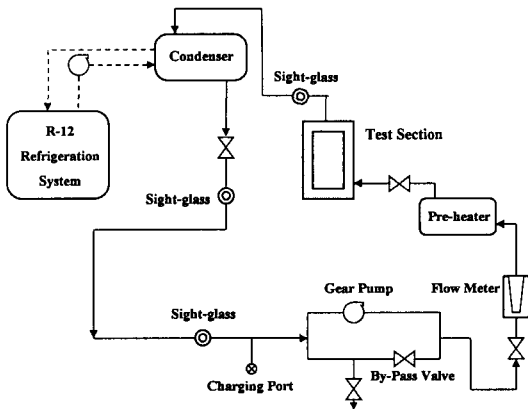


Fig. 2 Schematic of the experimental apparatus.

the test section is shown in Fig. 3. The apparatus and the test section were made similar to those used by Gupte and Webb.⁽¹⁰⁾ Refrigerant enters at the bottom of the test section at a known vapor quality. Heat is supplied to the tubes in the tube bundle by cartridge heaters. The two-phase mixture leaves the test section and goes to the condensers. Three condensers having 7.5 kW cooling capacity each are connected in parallel. The sub-cooled liquid then pass through a dryer, and goes to the magnetic pump having 1 gpm capacity. The mass flow meter [Micromotion DN25S-SS-1] is placed between the magnetic pump and the pre-heater to measure the mass flow rate. Heat is supplied to the pre-heater to obtain a known vapor quality. The two-phase mixture enters the test section through the feeder tubes located at the bottom of the tube bundle.

Heat input to the pre-heater determines the inlet vapor quality, which can be controlled independently. Since, the liquid loop is complete by itself, the mass flow rate can be controlled independently. Finally, the heat flux to the test tubes can be varied by regulating the line voltage to tubes. Thus, the apparatus was designed to control the vapor quality, mass velocity and heat flux independently.

Figures 3 and 4 show the details of the test section and the instrumented tube, respectively.

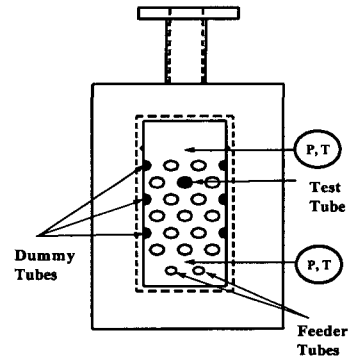


Fig. 3 Details of the test section.

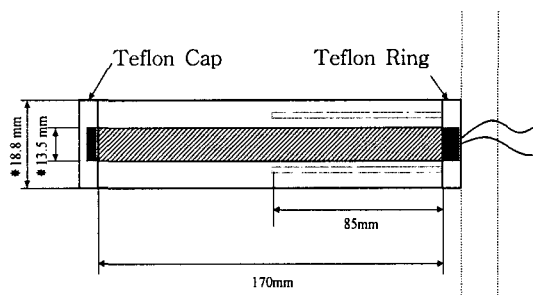


Fig. 4 Detail sketch of the test tube.

The test tubes were specially made from thick-walled copper tubes of 18.8 mm outer diameter and 13.5 mm inner diameter. The length of the test tube was 170 mm. Cartridge heaters of 13.45 mm diameter and 180 mm long were inserted into the test tubes. The heaters were specially manufactured to contain 170 mm long heated section (same length as that of the test tubes) and two 5 mm long unheated end sections. To minimize the heat loss, the unheated sections were covered with Teflon caps and Teflon rings as illustrated in Fig. 4. Before insertion, the heaters were coated with thermal epoxy to enhance the thermal contact with the tubes. The heaters were screwed into the back flange of the test section to form a staggered array of an equilateral triangular pitch of 23.8 mm. For that purpose, the heaters were specially manufactured to contain a male screw at one end. Heat was supplied to all the tubes except for those at the bottom row — its role was to develop flow in the tube bundle.

The instrumented tube was located at the center of the fifth row from the bottom. Figure 4 shows the cross section of the instrumented tube. The same tubes as those used by Kim and Choi⁽¹¹⁾ for the pool boiling test were used in the present study. The tubes have four thermocouple holes of 1.0 mm drilled to the center of the tube. Copper-constantan thermocouples of 0.3 mm diameter per wire were inserted into the holes to measure the tube wall temperature. Before insertion, the thermocouples were coated with a thermal epoxy [Chromalox HTRC] to provide good thermal contact with the tube wall. The thermal conductivity of the epoxy is close to that of aluminum. The steady state heat conduction equation was used to correct for the conduction temperature drop between the thermocouple and the boiling surface.

Saturation temperatures were measured at the top and the bottom of the tube bundle. Calibrated pressure transducers were also used to measure the saturation pressure at the same location. During the experiment, the saturation temperature calculated from the measured pressure was compared with the measured temperature, and they agreed within 0.2°C. The measured temperatures were used for data reduction. For convective boiling, the saturation temperature decreases along the flow passage due to the pressure loss. For the present experiment, the decrease was on the order of 0.5°C. The saturation temperature at the instrumented tube was determined by linear interpolation of the top and bottom temperatures.

3. Experimental procedures

Before beginning the experiment, the apparatus was checked for possible leakage. The apparatus was kept under vacuum for 24 hours, and the pressure rise was less than 10 kPa. While charging the system, a small amount of refrigerant was first introduced into the system. The system was then evacuated by a va-

cuum pump. This procedure was repeated several times before charging the system. Liquid refrigerant was introduced into the system from an inverted refrigerant drum to prevent any trapped gas in the drum entering the system. The absence of non-condensable gases was further confirmed by noting the agreement between the saturation temperature and the measured pressure in the test section.

Convective and pool boiling data were taken at two saturation temperatures, 4.4°C and 26.7°C. The mass velocity was varied from 8 kg/m²s to 26 kg/m²s, heat flux from 10 kW/m² to 40 kW/m² and vapor quality from 0.1 to 0.9. Data were taken first varying the vapor quality, the heat flux, and then the mass flux, all in a decreasing manner. The vapor quality at the instrumented tube location was determined from equation (1).

$$x = \left[\frac{Q_p + NQ_H}{\dot{m}_r} - c_{pr}(T_{p,sat} - T_{p,in}) \right] \quad (1)$$

Here, Q_p is the heat supplied to the pre-heater, Q_H is the heat supplied to a single heater in the test section, and N is the number of active heaters upstream of the instrumented tube. The test section and the pre-heater were heavily insulated to minimize the heat loss to the environment.

The heat transfer coefficient (h) was determined by the heat flux (q'') over wall superheat ($T_w - T_{sat}$). Calculations of q'' and h were based on the envelope area, defined by the heated length (170 mm) multiplied by the tube outside perimeter. The input power to the heater was measured by a precision watt-meter [Chitai 2402A] and the thermocouples were connected to the data logger [Fluke 2645A]. The pressure transducers were also connected to the data logger. The thermocouples and the transducers were calibrated and checked for repeatability. The calculated accuracy of the temperature mea-

surement was $\pm 0.10^\circ\text{C}$, the heat flux measurement $\pm 0.5\%$, the mass velocity measurement $\pm 1\%$ and the vapor quality measurement $\pm 2\%$. An error analysis was conducted following the procedure proposed by Kline and McClintock.⁽¹²⁾ The uncertainty in the heat transfer coefficient was estimated to be $\pm 2\%$ at the maximum heat flux (40 kW/m^2) and $\pm 8\%$ at a low heat flux (10 kW/m^2).

4. Results and discussions

4.1 Single tube test

Before the bundle test, heat was supplied to

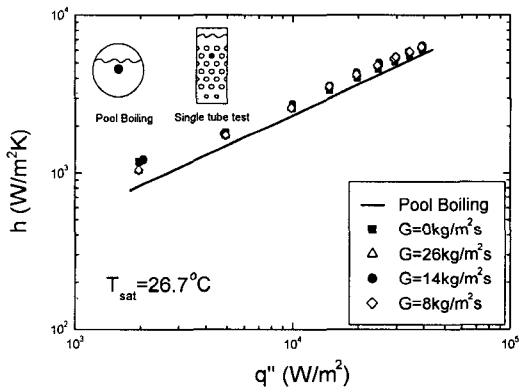


Fig. 5 Heat transfer coefficients for the single tube flow boiling at $T_{sat}=26.7^\circ\text{C}$.

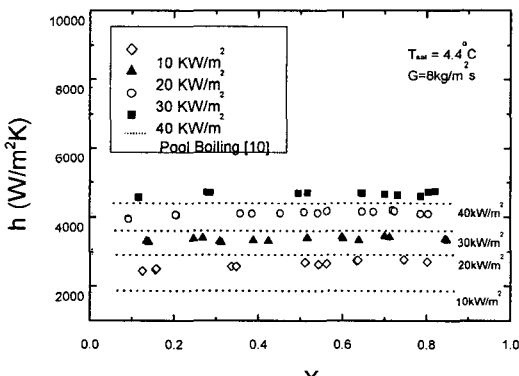


Fig. 6 Heat transfer coefficients for the bundle flow boiling at $G=8\text{ kg/m}^2\text{s}$ and $T_{sat}=4.4^\circ\text{C}$.

the instrumented tube with the other tubes inactive. The heat transfer coefficients are shown in Fig. 5. This figure shows that the effect of mass velocity is insignificant. The pool boiling test data⁽¹¹⁾ are compared with the present single tube data, and they agree each other. This suggests that the effect of the neighbouring tubes on the pool boiling is negligible.

4.2 Bundle test

Figure 6 shows the test results at $T_{sat}=4.4^\circ\text{C}$ and $G=8\text{ kg/m}^2\text{s}$. The heat transfer coefficient increases as the heat flux increases, and is almost independent of the quality. In Fig. 7,

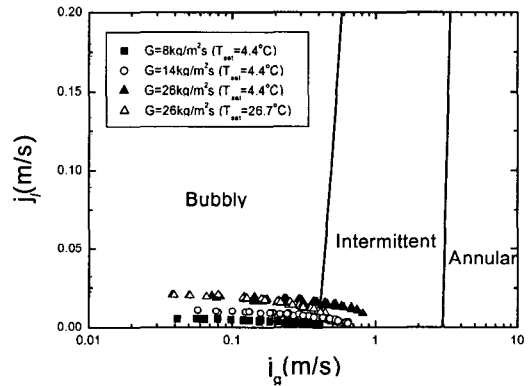


Fig. 7 The present data plotted in Noghrehkar et al's⁽¹³⁾ flow regime map.

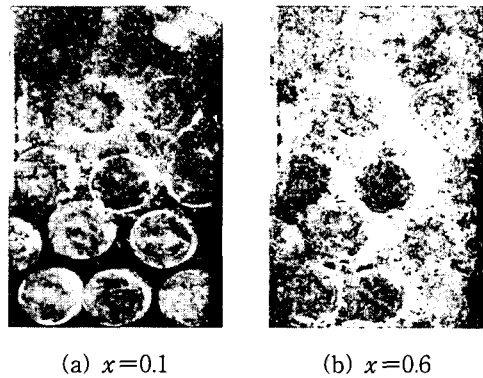


Fig. 8 Photos Showing the two-phase flow in the tube bundle at $q''=40\text{ kW/m}^2$, $G=26\text{ kg/m}^2\text{s}$.

the present data are plotted on the flow regime map of Noghrehkar et al.⁽¹³⁾ The flow regime map was developed from the air-water two-phase flow data in a staggered bundle. Figure 7 shows that most of the present data pertain to a bubbly flow regime, which agree with the results from visual observation. The photos taken at $q''=40\text{ kW/m}^2$, $x=0.1$ and $x=0.6$, shown in Fig. 8 supports the flow regime. For an in-tube flow boiling, flow becomes annular as quality increases. For the bundle boiling, on the contrary, flow remains bubbly even at a high quality. The independency of the heat

transfer coefficient with quality may be related with the prevailing bubbly flow even at a high quality. In Fig. 6, the pool boiling heat transfer coefficients are also shown. The flow boiling heat transfer coefficients are 6% to 40% higher than those of the pool boiling.

In Fig. 9, the data at $G=14\text{ kg/m}^2\text{ s}$ are shown. The heat transfer coefficient shows a similar trend as that of the $G=8\text{ kg/m}^2\text{ s}$ except for the low heat flux ($q''=10\text{ kW/m}^2$) and low quality region. At that region, the heat transfer coefficient increases with quality. In Fig. 10, the data at $G=26\text{ kg/m}^2\text{ s}$ are shown.

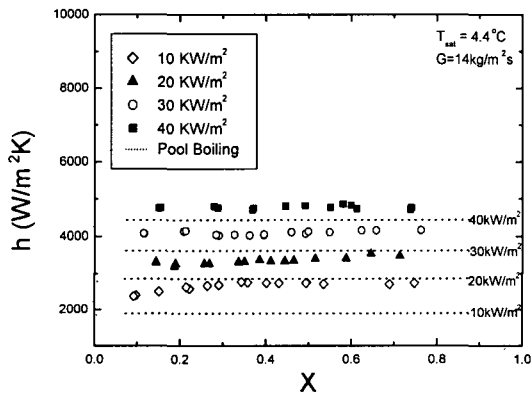


Fig. 9 Heat transfer coefficients for the bundle flow boiling at $G=14\text{ kg/m}^2\text{ s}$ and $T_{sat}=4.4^\circ\text{C}$.

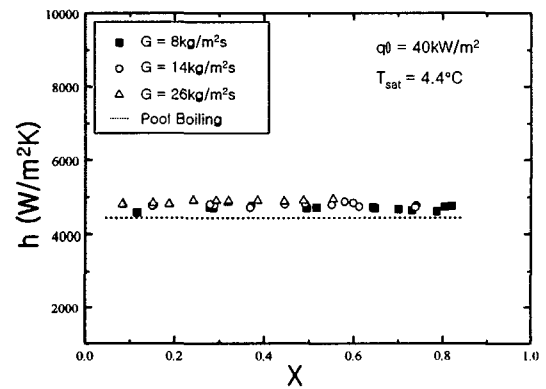


Fig. 11 Heat transfer coefficients for the bundle flow boiling at $q''=40\text{ kW/m}^2$ and $T_{sat}=4.4^\circ\text{C}$.

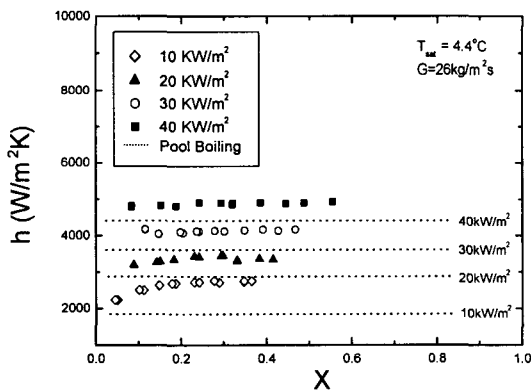


Fig. 10 Heat transfer coefficients for the bundle flow boiling at $G=26\text{ kg/m}^2\text{ s}$ and $T_{sat}=4.4^\circ\text{C}$.

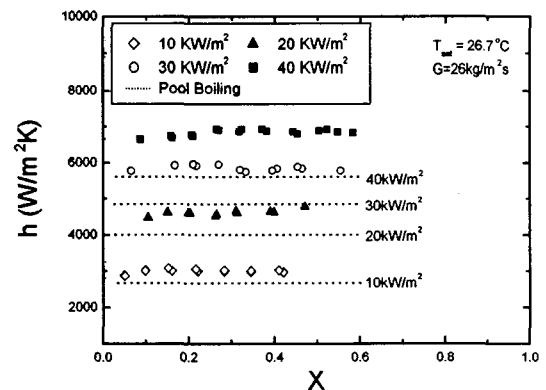


Fig. 12 Heat transfer coefficients for the bundle flow boiling at $G=26\text{ kg/m}^2\text{ s}$ and $T_{sat}=26.7^\circ\text{C}$.

A similar trend as $G=14 \text{ kg/m}^2\text{s}$ is noted. In Fig. 11, the heat transfer coefficients at $q'' = 40 \text{ kW/m}^2$ are shown. This figure reveals that the effect of mass velocity is negligible. The present experiment was conducted for $8 \text{ kg/m}^2\text{s} \leq G \leq 26 \text{ kg/m}^2\text{s}$. For a larger mass velocity, we expect the effect of mass velocity. The operating mass velocity of a turbo-refrigerator is between $10 \text{ kg/m}^2\text{s}$ and $20 \text{ kg/m}^2\text{s}$.⁽¹⁴⁾

In Fig. 12, the data at $G=26 \text{ kg/m}^2\text{s}$ and $T_{\text{sat}} = 26.7^\circ\text{C}$ are shown. The flow boiling heat transfer coefficient is 6% to 23% larger than that of the pool boiling. In Fig. 13, the data at 4.4°C are compared with those at 26.7°C . The mass flux is $26 \text{ kg/m}^2\text{s}$. This figure shows that the heat transfer coefficient increases with the saturation temperature. A similar trend was noted for the pool boiling test.⁽¹¹⁾

The present data are compared with the modified Chen correlation following the suggestion by Webb and Gupte.⁽⁸⁾ Chen's flow boiling model is as follows.

$$h = Sh_{nb} + Fh_{fc} \quad (2)$$

where h_{nb} is the nucleate boiling heat transfer coefficient and h_{fc} is the forced convective heat transfer coefficient obtained for the liquid-only

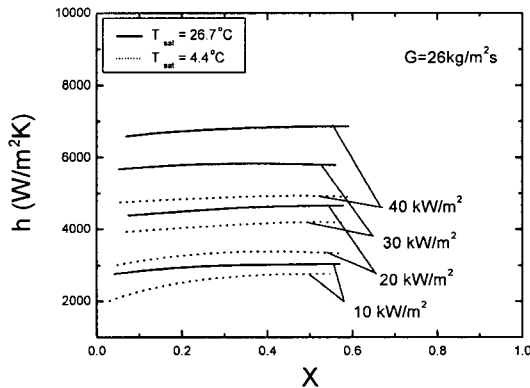


Fig. 13 Heat transfer coefficients for the bundle flow boiling at $G=26 \text{ kg/m}^2\text{s}$.

flow in a bundle. For a smooth tube bundle, h_{nb} may be obtained from the experimental data or a correlation such as Cooper.⁽¹⁵⁾ The h_{fc} may be obtained from Zukauskas⁽¹⁶⁾ correlation. In a forced convective boiling, the nucleate boiling is suppressed as the quality increases by the thinning of the liquid film on the wall. The suppression factor S for the bundle boiling has been reported by Bennet and Chen.⁽¹⁷⁾ As the quality increases, the flow velocity increases, and the effect of forced convection also increases. The increase is commonly represented by the F factor. The correlations for the F factor applicable to a bundle have been suggested by Bennet and Chen,⁽¹⁷⁾ Jensen and Hsu⁽³⁾ and Polley et al.⁽¹⁾ Gupte and Webb⁽⁸⁾ recommended Bennet and Chen correlation.

$$S = \left(\frac{k}{Fh_{fc}X_0} \right) \left[1 - \exp\left(-\frac{Fh_{fc}X_0}{k} \right) \right] \quad (3)$$

$$X_0 = 0.041 \left[\frac{\sigma}{g(\rho_l - \rho_g)} \right]^{0.5} \quad (4)$$

$$F = \left(\phi_l^2 \frac{\text{Pr} + 1}{2} \right)^{0.327} \quad (5)$$

In Fig. 14, the data at $G=8 \text{ kg/m}^2\text{s}$ are com-

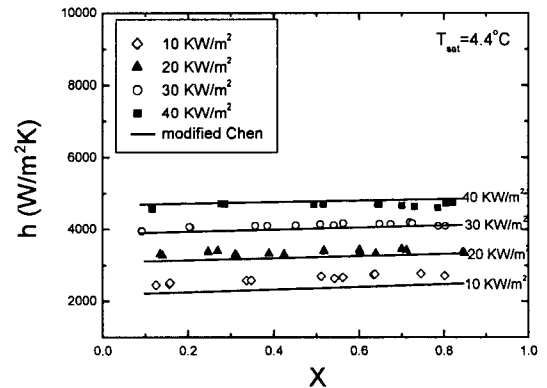


Fig. 14 The present data ($G=8 \text{ kg/m}^2\text{s}$) compared with the modified Chen correlation.

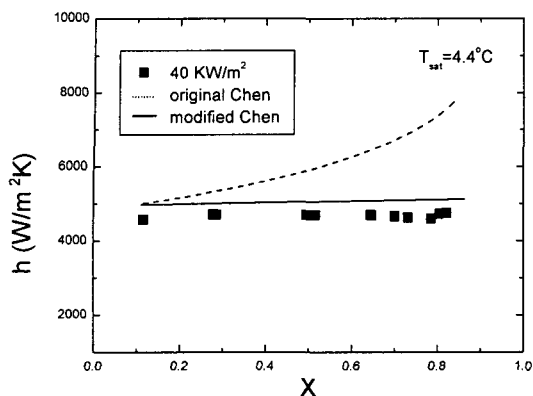


Fig. 15 The present data ($G=8 \text{ kg/m}^2\text{s}$, $q'' = 40 \text{ kW/m}^2$) compared with the original and the modified Chen correlations.

pared with the predictions. This figure shows the good agreement is obtained. In Fig. 15 the present data are compared with the original Chen correlation developed from the in-tube flow boiling data. The effect of quality is not correctly predicted. This suggests that different S and F factors should be used for different geometries. In Fig. 16, the present data are compared with the modified Chen correlation, which agree with in $\pm 30\%$.

5. Conclusions

In this study, flow boiling experiments were performed using R-134a on a plain tube bundle. Tests were conducted for the following range of variables; quality from 0.1 to 0.9, mass flux from $8 \text{ kg/m}^2\text{s}$ to $26 \text{ kg/m}^2\text{s}$ and heat flux from 10 kW/m^2 to 40 kW/m^2 . Listed below are major findings.

(1) The heat transfer coefficients were strongly dependent on the heat flux. However, they were almost independent on the mass flux or quality.

(2) The data are compared with the modified Chen model, which satisfactorily ($\pm 30\%$) predicted the data. Original Chen model, however, did not adequately predict the effect of quality.

(3) The heat transfer coefficients of the tube

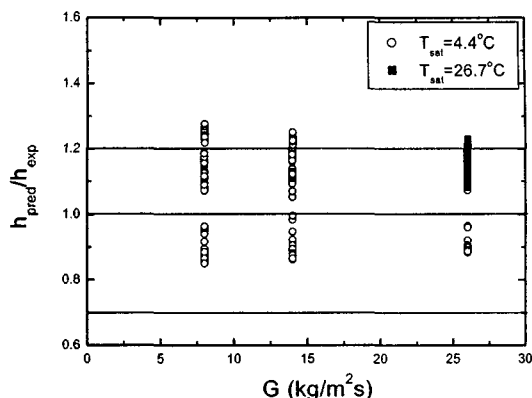


Fig. 16 Comparison of the present data with the modified Chen correlation.

bundle were 6~40% higher than those of the single tube pool boiling.

Acknowledgement

The financial support from 1998 Energy R & D fund is appreciated.

References

1. Polley, G. T., Ralston, T. and Grant, I. D. R., 1980, Forced Crossflow Boiling in an Ideal In-Line Tube Bundle, ASME Paper, 80-HT-46.
2. Hwang, T. H. and Yao, S. C., 1986, Forced Convective Boiling in Horizontal Tube Bundles, Int. J. Heat Mass Transfer, Vol. 29, No. 5, pp. 785-795.
3. Jensen, M. K. and Hsu, J.-T., 1987, A Parametric Study of Boiling Heat Transfer in a Tube Bundle, Proc. 1987 ASME-JSME thermal Engineering Joint Conf., Vol. 3, pp. 133-140.
4. Reinke, M. J. and Jensen, M. K., 1987, A Comparison of Boiling Heat Transfer Two-Phase Pressure Drop between an Inline and a Staggered Tube Bundle, in Boiling and Condensation in Heat Transfer Equipment, E. G. Ragi et al. (eds.), ASME, HTD-Vol.

- 85, pp. 41-50.
5. Cornwell, K. and Scoones, D. S., 1988, Analysis of Low Quality Boiling on Plain and Low Finned Tube Bundles, IMechE/ICHEME, Proc. 2nd UK Heat Transfer Conf., Vol. 1, pp. 21-32.
 6. Jensen, M. K., Trewin, R. R. and Bergles, A. E., 1992, Crossflow Boiling in Enhanced Tubes, Proc. Engineering Foundation Conf. on Pool and External Flow Boiling, ASME, pp. 373-379.
 7. Webb, R. L. and Chien, L. H., 1994, Correlation of Convective Vaporization on Banks of Plain Tubes Using Refrigerants, Heat Transfer Engineering, Vol. 15, No. 3, pp. 57-69.
 8. Webb, R. L. and Gupte, N. S., 1992, A Critical Review of Correlations for Convective Vaporization in Tubes and Tube Banks, Heat Transfer Eng., Vol. 13, No. 3, pp. 58-81.
 9. Chen, J. C., 1966, A Correlation for Boiling Heat Transfer to Saturated Fluids in Convective Flow, Ind. Eng. Chem. Process Design Dev., Vol. 5, No. 3, pp. 322-329.
 10. Gupte, N. S. and Webb, R. L., 1995, Convective Vaporization Data for Pure Refrigerants in Tube Banks, HVAC & R Research, Vol. 1, No. 1, pp. 48-60
 11. Kim, N-H. and Choi, K-K., 2001, Nucleate Pool Boiling of Structured Enhanced Tubes Having Connecting Gaps, printing in Int. J. Heat Mass Trans, Vol. 44, pp. 17-28.
 12. Kline, S. J. and McClintock, F. A., 1953, The Description of Uncertainties in Single Sample Experiments, Mechanical Engineering, Vol. 75, pp. 3-9.
 13. Noghrehkar, R., Kawaji, M. and Chan, A. M. C., 1999, An Experimental Study of Two-Phase Flow Regimes In-Line and Staggered tube Bundles Under Cross-Flow Conditions, Int. J. Multiphase Flow.
 14. Gupte, N. S. and Webb, R. L., 1992, Convective Vaporization of Refrigerants in Tube Banks, ASHRAE Transactions; Symposia, pp. 411-424.3.
 15. Cooper, M. G., 1984, Saturation Nucleate Pool Boiling—a Simple Correlation, International Chemical Engineering Symposium Series, No. 86, pp. 785-792.
 16. Zhukauskas, A., 1972, Heat transfer from Tubes in Cross Flow, in Advances in Heat Transfer, J.P. Hartnett and T.F. Irvine (eds.), Vol. 8, Academic Press, New York.
 17. Bennett, L. and Chen, J. C., 1980, Forced Convective Boiling In Vertical Tubes for Saturated Pure Components and Binary Mixtures, AIChE J., Vol. 26, No. 3, pp. 454-461.